

Central European Journal of Chemistry

Temperature-induced phase transition; Polymorphism in BP2 SAMs on Au(111)

Research Article

Waleed Azzam

Department of Chemistry, Tafila Technical University, P.O.Box 179, Tafila, Jordan

Received 10 November 2008; Accepted 18 June 2009

Abstract: Self-assembled monolayers (SAMs) of ω -(4'-methylbiphenyl-4-yl)ethanethiol (CH $_3$ (C $_6$ H $_4$) $_2$ (CH $_2$) $_2$ SH, BP2) prepared at different temperatures on Au(111) substrates were investigated using scanning tunneling microscopy (STM). Also, the effect of the incubation time of the gold substrate in the thiol solution was examined. The STM results showed that samples prepared at room temperature were significantly different from those prepared at elevated temperatures in their surface morphology, space group and size of unit cell. The micrographs of samples prepared at higher temperatures revealed a pronounced and progressive increase in the size of the well-known etch-pits at the expense of their density with increasing preparation temperature (but the increase did not continue for SAMs prepared at 348 K). The average domain size was found to increase significantly with increasing preparation temperature. In addition, polymorphism was observed in BP2 SAMs at all investigated temperatures. This study has demonstrated that solution temperature and incubation time are key factors controlling the two-dimensional SAM structure of BP2 molecules.

Keywords: SAM • STM • Thiol • Temperature-induced phase transition • Immersion time

© Versita Warsaw and Springer-Verlag Berlin Heidelberg.

1. Introduction

The study of self-assembled monolayers (SAMs) has attracted very widespread interest, due to their potential for a large array of applications in different fields such as electronic devices [1-3] chemical sensors [4,5], corrosion protection [6], lithography [5,7], or biocompatible coatings [8]. The most commonly studied SAM system is organothiols on gold surfaces due to their ease of preparation, their good stability even in air, the absence of significant gold oxidation under ambient conditions, and the extremely high degree of ordering present at the Au(111)-S interface. Recently, SAMs of aromatic thiols have been the focus of concentrated interest as they provide an interesting alternative to alkane-based thiol SAMs [9-34]. Increasing interest in these systems can be attributed to the physical and chemical properties of aromatic thiols. First, they

have an azimuthally anisotropic structure, which drives the molecules to an ordered alignment through $\pi\text{-}\pi$ stacking. The intermolecular interactions are stronger than those of alkanethiols, leading to different molecular packing structures. Second, they have higher electrical conductance than alkanethiols [35,36] because the electrons are delocalized in the benzene rings than localized in the alkane chains. Finally, it is easier to attach different functional groups to the opposite end in the molecular structure of the aromatic thiols in a SAM. Consequently, aromatic thiols have been considered as candidates for a number of applications including molecular wires [37] and electron-transfer [5] promoters for electroanalytical sensors.

For molecular electronic applications it is an important issue to achieve fabrication and control of the two-dimensional structures of aromatic thiol SAMs down to the length scale of molecular dimensions. Several SAM properties are seriously dependent on

details of the SAM structure at this scale. This is clearly emphasized in previous studies [38,39], where molecular orientation, intermolecular interactions, head-group substrate bonding, and SAM defects such as etch-pits were found to have affected the electronic properties of the SAM. Accordingly, it is crucial to achieve a better understanding of the structure and stability of various phases at room and elevated temperatures. Previous studies have shown that ordered SAMs on Au(111) are the result of the intermolecular interactions between the adsorbates within the SAM and the sulfur-Au interaction. Unlike alkanethiol-based SAMs, whose structure is largely independent of the chain length, the structure and the ordering mechanism of aromatic SAMs is more complicated. A conspicuous example of this complexity is found in SAMs generated from biphenyl derivatives BPn $(CH_3(C_6H_4)_2(CH_2)_2SH)$ [32,40] and terphenyl derivatives TPn ((C₆H₄)₃(CH₂)_nSH) [23]. These films were found to exhibit a pronounced alternation in both molecular packing and orientation with changing the parameter n from odd to even. Moreover, such a distinct dependence on the number of -CH₂ units affects a number of film properties including electrochemical stability [41], stability toward exchange by other thiols [42], and electron irradiation [43]. The structure formed by the odd-numbered SAMs was found to be (2√3×√3)R30° structure. In contrast, the evennumbered SAMs were described by a much larger $(5\sqrt{3}\times3)$ structure with an area per molecule larger by about 25% compared to n=odd(32). However, these structures are not the only structures observed for aromatic thiols on Au(111). For example, a striped $(7 \times \sqrt{3})$ phase for 2-phenylmercaptan [33] and striped $(15\times\sqrt{3})$ and $(2\times\sqrt{3})$ structures for benzylmercaptan [34] were recently observed on Au(111). Recently the SAMs from ω-(4'-methylbiphenyl-4-yl)ethanethiol (CH₃(C₆H₄)₂(CH₂)₂SH), BP2 have been studied [44]. At low temperature, the $(5\sqrt{3}\times3)$ structure was observed [40,44]. Upon annealing, a phase transition from the low temperature (5 $\sqrt{3}$ ×3) structure, common to all SAMs prepared from the n=even homologues in the above series of BPn, to a new (2√3×2) structure was observed. In another study [45], two new structures with rectangular (4×6√3) lattices have been identified for BP2 SAMs on Au(111) [45]. It is obvious that there are some discrepancies between the previous studies concerning the structures formed by BP2 molecules on Au(111).

Indeed, there are very large questions still open to debate, about the mechanistic details of the chemisorption process of aromatic thiols on Au(111) such as the structure of the Au(111)-S interface. Nevertheless, the overall result is the breaking of the –S-H bond to form a thiolate species chemically bound to the gold substrate.

There is general agreement that the 24 hour immersion period of the gold substrate into the thiol solution allows the molecular film to assemble into the final crystalline type solid phase, and in this process the physisorbed and chemisorbed contaminants are desorbed from the surface into solution. These uncertainties and apparent contradictions about the BP2-adlayer, raise several questions in relation to the effects of incubation time and of the temperature of the thiol solution during the adsorption process.

The purpose of the present paper is to present a relationship between the molecular arrangement of the BP2 adsorbates and the preparation conditions such as temperature and incubation times. SAMs of BP2 prepared at different temperatures for different immersion times were examined using STM. This study shows that BP2 molecules adsorb spontaneously on the Au(111) surface to form different structural phases that coexist on Au(111).

2. Experimental Section

2.1. Chemicals

BP2 was synthesized and purified using previously described procedures [40]. Ethanol (Baker), acetone (Baker), and chloroform (Baker) were used as received.

2.2. Sample Preparation 2.2.1. Substrates

For the STM investigations, first a freshly cleaved sheet of mica was heated to 370°C for about 48 h inside the evaporation apparatus to remove residual water contained between the mica sheets. Subsequently, 100 nm of Au were deposited at a substrate temperature of 370°C and a pressure of approximately 10⁻⁷ mbar. After deposition, the substrates were allowed to cool, and the vacuum chamber was vented with purified nitrogen (99.99%). Between substrate preparation and SAM formation, the substrates were stored in an argon atmosphere. Immediately before the SAM preparation, the substrates were flame-annealed using a butaneoxygen flame. This procedure yielded Au substrates with well-defined terraces exhibiting a (111)-oriented surface. The terraces are separated by steps of monatomic height and have sizes in excess of 100 nm.

2.2.2. Preparation of the BP2 SAMs

BP2 monolayers on Au(111) substrates were prepared by immersing the gold substrates into dilute ethanolic solutions (100 μ M) of the thiols for different periods (see text) at different temperatures of thiol-solution (see

text). The substrate was removed from the solution and rinsed carefully with pure ethanol, acetone, chloroform and again ethanol. Finally the substrates were dried in a stream of dry nitrogen.

2.3. Structural Investigations

STM data were obtained using a commercial Nanoscope IIIa Multimode microscope (Digital Instruments, Santa Barbara, CA) equipped with a type "E" scanner. The tips were prepared by cutting a Pt/Ir (80:20, Chempur) wire mechanically. All STM micrographs were recorded in air at room temperature in constant-current mode.

3. Results

3.1. SAMs Prepared at RT

3.1.1. Short-Immersion Time

Figs. 1a-d show constant-current STM images recorded for an Au(111)-substrate, which has been immersed for 2 h in 100 μ M solution of BP2 in ethanol at room temperature. The STM image displayed in Fig. 1a reveals several Au terraces that are separated by monoatomic gold steps. Within the terraces, numerous etch-pits (depressions) with diameters of 2-7 nm and

a depth corresponding to that of monatomic steps on Au(111) (2.4 Å) are observed. Fig. 1b shows that the etch-pits are not randomly distributed on gold surface; rather, they are arranged in a regularly spaced fashion. The inset shown in Fig. 1b exhibits a small area taken from the STM image displayed in Fig. 1b. Along the lines A and B (labeled in the inset), the etch-pits are separated by distances of 13±2 and 7±1 nm, respectively.

In addition to the etch-pits, many dark patches are observed within the terraces (see the black circles in Fig.1c). The depth of these dark patches was determined from several STM images to be 0.5-1 Å. This value is much less than the height of monoatomic gold (2.4 Å), which is characteristic for the depth of the etch-pits. Consequently, these dark-patches cannot be identified as regions where gold atoms are missing in the first layer of the gold surface. Similar dark patches have been recently observed on BP2 modified gold surface(16). The patches have been attributed to a substantial lattice mismatch between the ideal structure for BP2 adsorbate adlayers and the underlying gold substrate. Higher resolution images such as are shown in Figs. 1d and f reveal that the dark patches are not devoid of BP2 molecules. On the contrary, they are filled with molecules having almost the same molecular

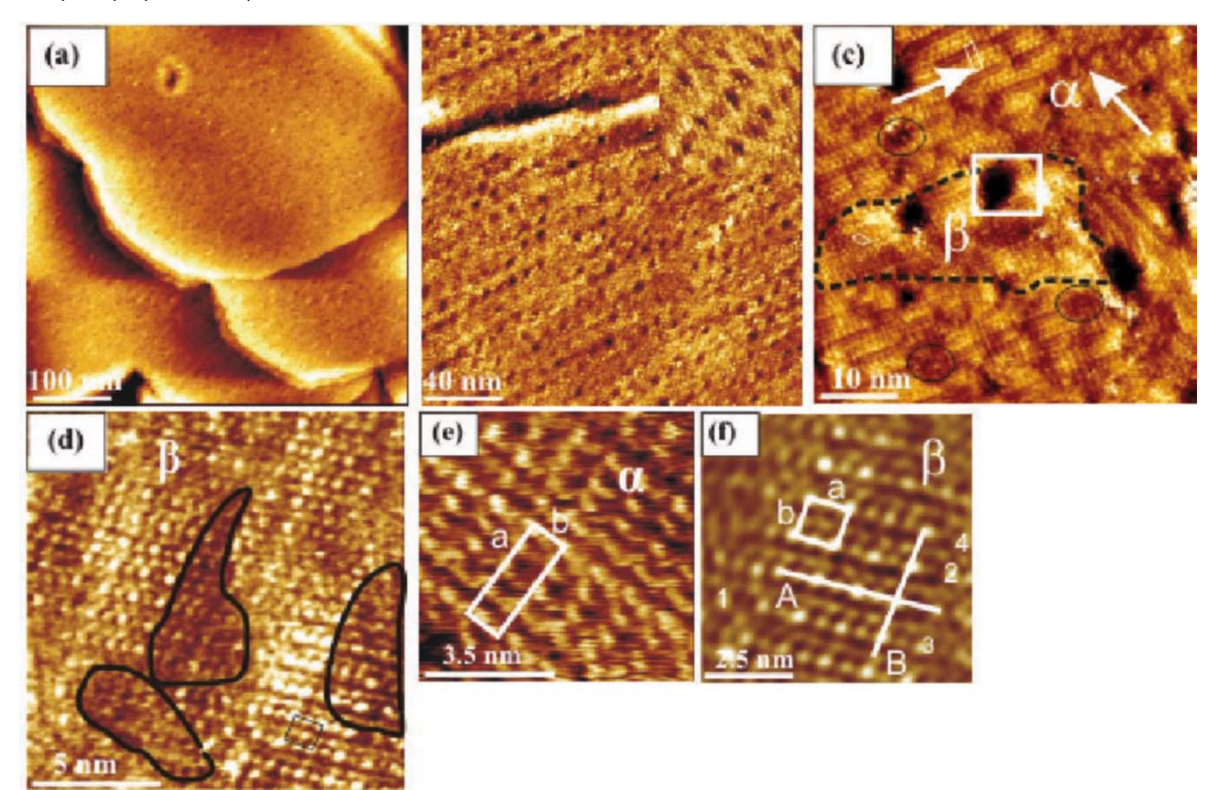


Figure 1. Constant-current images for a Au(111)-substrate, which has been immersed for 2 h into 100 µM solution of BP2 in ethanol RT. The unit cell of the rectangular (5√3×3) structure is marked in (c) and (e). The unit cell of the rectangular (2√3×3) structure is marked by the rectangular in (d) and (f). Tunneling parameters: (a) U= 1000 mV; I= 148 pA, (b) U= 850 mV; I= 148 pA, (c) U= 550 mV; I= 148 pA, (d) U= 550 mV; I= 130 pA, (e) U= 530 mV; I= 148 pA, and (f) U= 530 mV; I= 148 pA.

arrangement as that found in their neighbourhood (see the region confined by the black line in Figs. 1d and f). Zooming in onto one of the dark-patches (see Fig. 1f), shows clearly that the organothiolate adlayer within the dark patches is laterally displaced (expands or shrinks) relative to the structure in the surrounding neighbourhood (see molecules numbered 1-4) by about 0.5 Å. This slight difference between the adlayer structures inside and outside the dark patches is attributed to a mismatch between the adsorbate and the underlying substrate. To guide the eyes of the reader, etch-pits and dark patches are marked in Fig. 1c with white squares and black circles, respectively.

Fig. 1c and d, show images of the BP2 layer on Au(111) at molecular resolution. We observed that BP2-SAMs generated on Au(111) after two hours of immersion actually have two distinct mixed phases (α and β , hereafter). In Fig. 1c, the α -phase with rod-like domains has a rectangular structure. The length of the rod-like ordered domains ranged from a few nanometers to approximately 25 nm. The second phase is the β -phase with a rectangular unit cell. The length of the β -phase domains is between 5 to 15 nm. In Fig. 1c, the region confined by a dashed loop shows the β -phase. The rest of the image shows the α -phase. In Fig. 1c, the arrows show two rotational orientations of α -phase domains separated from each other by about 120°.

A molecular resolution image showing α-phase is displayed in Fig. 1e. For α-phase, the measured lattice constants are a=25±1 Å and b=8.6±0.5 Å and the angle between the lattice vectors is 90±2°. A possible model structure is $(5\sqrt{3}\times3)$ structure (a= $5\sqrt{3}a_{AII}$, where a_{Au}=2.89 Å). High-resolution STM images for this phase reveal the presence of eight molecules in each unit cell, yielding an area of 27.05 Å² per molecule. A variation in the height of the adsorbed molecules within the $(5\sqrt{3}\times3)$ unit cell is observed. A model representing the $(5\sqrt{3}\times3)$ structure is displayed in Fig. 1f. The variation in topographic heights of the adsorbed molecules can be attributed to the adoption of different sulfur adsorption sites on Au(111). The α-phase is well-known from our previous studies of BPn SAMs, and is characteristic of BPn systems with an even number of CH₂ units prepared from solutions at room temperature or a little higher [32,40]. The β-phase is shown in the STM images displayed in Figs. 1c, d and f. A more detailed explanation of this phase will be provided in the discussion of SAMs of BP2 prepared at elevated temperatures. Meanwhile, the lines labeled A and B in the STM image in Fig. 1f, indicate alternate rows of molecules. Every second row of molecules exhibits the same height, corresponding to a unit cell with a=10±0.5 Å and b=9±0.8 Å, respectively. The molecules are separated by an intermolecular distance of about $5\,\text{Å}$ along the lines A and B. The angle between the lattice vectors of the unit cell amounts to $90\pm3^{\circ}$. These values fit nicely to a rectangular $(2\sqrt{3}\times3)$ structure. The high-resolution image of BP2 in Fig. 1f shows the presence of four molecules per unit cell, corresponding to an area per molecule of 21.6 Ų. The rectangular box depicted in Fig. 1f marks the $(2\sqrt{3}\times3)$ unit cell. A model representing the $(2\sqrt{3}\times3)$ structure is displayed in Fig. 4c.

3.1.2. Long-Immersion Times

Figs. 2a-d show constant-current STM images recorded for an Au(111)-substrate, which has been immersed for 24 h in 100 µM solution of BP2 in ethanol at room temperature. In Fig. 2a, the surface morphology of BP2- SAMs after 24 h of immersion looks similar to that observed for n-alkanethiols SAMs on Au(111) regarding the size, shape and depth (2.4 Å) of the etch-pits. The STM images shown in Figs. 2b and c show that the formation of the BP2 films after 24 h of immersion at RT is accompanied by the appearance of small islands having diameter of about 1-3 nm. These small and stationary bump-like features are 2.5 Å in height and randomly scattered over the surface. They are probably formed from gold-thiolate species that have peeled off and been pushed up from the film, and have then diffused to the nearest step-edge where they grow. The size of these islands indicates that each island is composed of only 1-5 thiolate species. The presence of these diffused species gives good information about the stability of the respective phases in the SAMs. The molecular arrangement within these SAMs is expected to be in growing process, which finally leads to a stable energetically preferred structure. The small islands are marked in the STM image by white circles.

An additional idiosyncratic feature of the SAM morphology is the presence of cloud-like features. Some of these features are indicated within black circles on the micrographs. Their height was measured at about 0.5 Å. In Fig. 2d, one can clearly see that these features are only sets of BP2 molecules rising slightly above their neighbors in topographical height. The clear inference is that molecules forming these features are using higher S-atom adsorption sites on the gold surface. From Fig. 2d, the height of the molecules within the cloud-like features is equal to the height of the adsorbate molecules located at the edges of the $(5\sqrt{3}\times3)$ unit cell of α -phase. Intermolecular distances within the cloud-like features are mostly not constant; these cloud-like features can therefore be identified as disorder regions. The presence of these features made it difficult for us to differentiate between the different phases coexisting in BP2-SAMs formed after one day of immersion period. The previous two α and β-phases could hardly be discerned in some

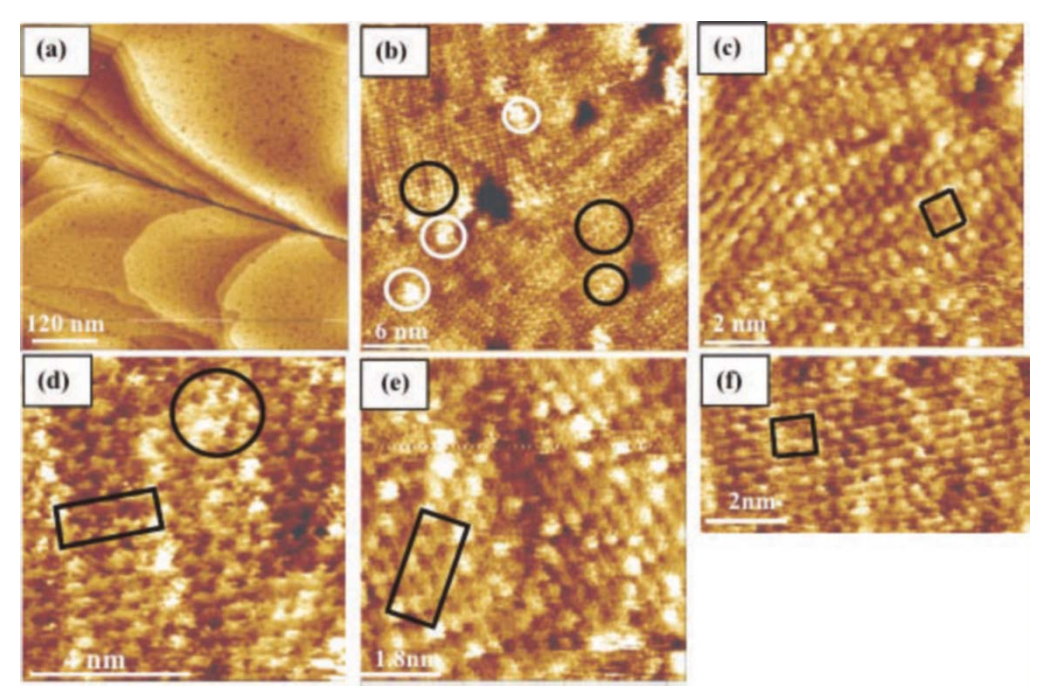


Figure 2. (a-d) Constant-current images for a Au(111)-substrate, which has been immersed for 24 h into 100 μM solution of BP2 in ethanol RT; (e-f) Constant-current images for a Au(111)-substrate, which has been immersed for 72 h into 100 μM solution of BP2 in ethanol RT. White circles in (b) confined regions showing the small elevated islands (height 2.5 Å) and black circles in (b) and (d) confined regions showing the clouds-like features. The unit cell of the (5√3×3) structure is marked by the rectangular in (d) and (e). The unit cell of the rectangular (2√3×3) structure is marked in (c) and (f). Tunneling parameters: (a) U= 950 mV; I= 450 pA, (b) U= 950 mV; I= 350 pA, (c) U= 550 mV; I= 130 pA, (d) U= 550 mV; I= 130 pA, (e) U= 530 mV; I= 150 pA, and (f) U= 530 mV; I= 150 pA.

of the STM images. The size of the ordered domains of both phases is small and does not exceed a few unit cells, as shown in Figs. 2c and d. We would like to point out that α –phase is the predominant one under these preparation conditions.

When the immersion time was increased to three days under the same conditions of temperature and concentration, no dramatic changes were observed: neither on the surface morphology at large-scale nor on the equilibrium structure at molecular-scale. Representative STM images confirming these observations are shown in Figs. 2e and f. Again, the $(5\sqrt{3}\times3)$ and $(2\sqrt{3}\times3)$ structures were resolved with predominance for the $(5\sqrt{3}\times3)$ structure.

3.2. SAMs Prepared at Elevated Temperatures *3.2.1. Short-and Long-Immersion Times at 333 K*

Samples prepared at 333 K (not shown) exhibited surface morphologies and film structures identical with those prepared at RT at all immersion periods. The α - and β -phases have been observed at different immersion times.

3.2.2. Short -Immersion Time at 343 K

Figs. 3a-f show constant current STM images recorded for an Au(111)-substrate, which has been immersed for

2 h in 100 µM solution of BP2 in ethanol at 343 K. In the large-scale images displayed in Figs. 3a and b, the STM micrographs show, in addition to the etch-pits, a large number of accidentally disseminated cracks. These cracks disconnect ordered domains. The depth of the cracks is about 1.5 Å. The numerical abundance of the etch-pits is very low but their size is large (about 50 nm in some cases). In a higher resolution image of a BP2 SAM (Fig. 3c), the cracks and the pits are clearly shown. In addition to the cracks and etch-pits, the micrograph features rows of missing molecules, indicated by a white arrow. In addition to the BP2-film defects, the SAM is characterized by the presence of the small islands (previously described in section 3.1.2) which have height of 2.4 Å (see Figs. 4a and b). Nearby, small pits having approximately the same size as the small-islands have also been observed. Some of these elevated-features and pits are indicated in the STM images by white and black circles, respectively.

The surface in Fig. 3c consists of ordered-rows with three-directional domain orientations, as indicated by the arrows on the image. In most cases, the angles between the domains are 60° or 120°, implying that the domain orientations were strongly affected by the hexagonal lattice of the Au(111) substrate. These ordered domains have an average size of 40-80 nm. Within the complexity

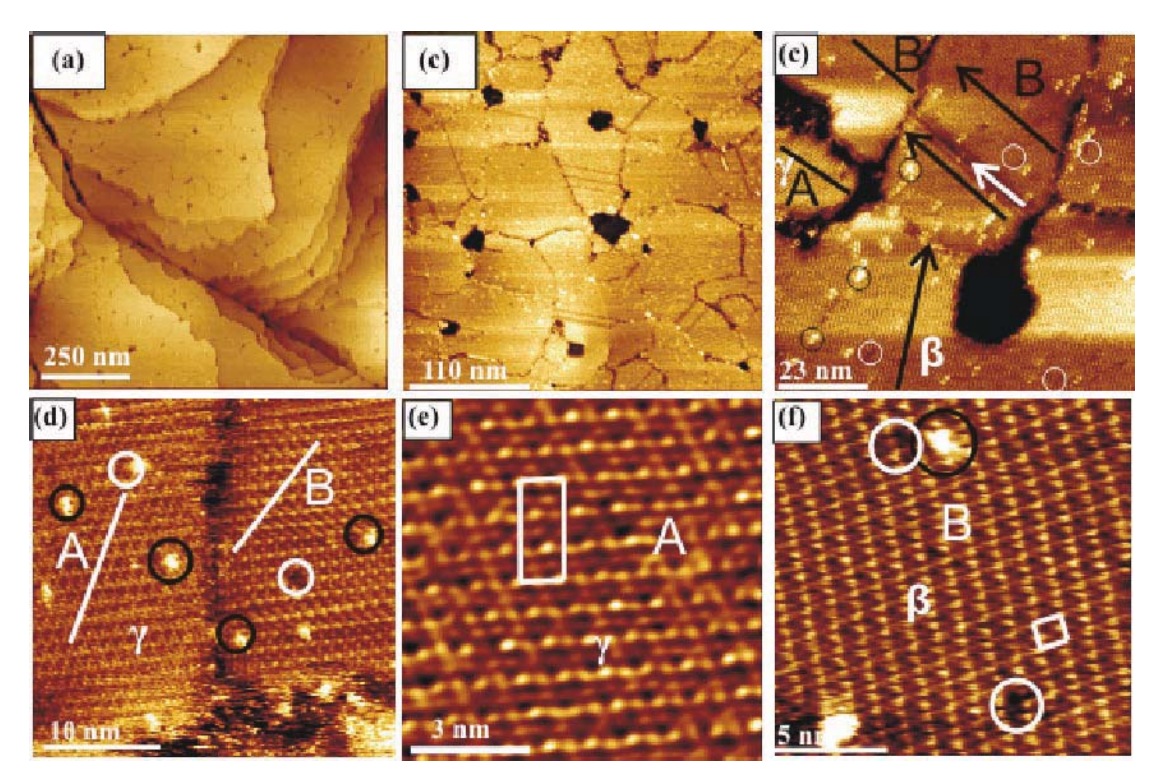


Figure 3. Constant-current images for a Au(111)-substrate, which has been immersed for 2 h into 100 μM solution of BP2 in ethanol 343 K. The arrows in (c) show the direction of the ordered domains. The regions surrounded by the black and white circles show the small-elevated islands and the nearby vacancy islands, respectively. The unit cell of the rectangular (5√3×4) and (2√3×3) structures are marked in (e) and (f), respectively. Tunneling parameters: (a) U= 1000 mV; I= 150 pA, (b) U= 1000 mV; I= 150 pA, (c) U= 530 mV; I= 150 pA, (d) U= 530 mV; I= 150 pA, (e) U= 530 mV; I= 148 pA, and (f) U= 530 mV; I= 148 pA.

already incorporated in such a three-directional structure it may seem difficult to discern whether there are different phases coexisting with each other. Actually, in some regions such as those marked by A and B, the ordered domains are separated from each other by an angle of 14±2°, strongly suggesting the presence of two different phases coexisting in the monolayer. Fig. 3d shows an expanded and higher-resolution image exhibiting both phases. Zoomed-in views showing the regions A and B are shown in Figs. 3e and f, respectively. The structural details of these phases observed in the regions A and B are displayed in Fig. 4. Firstly, we will discuss the molecular arrangement found in region B. The cross-sectional profiles in Fig. 4b taken along the lines A and B corresponding to the unit cell in Fig. 4a, show the periodicities of the BP2 molecules in the SAMs. The distance between the neighboring brighter spots (molecules) along the lines A and B amounts to 10±0.6 Å and 09±0.4 Å, respectively. The lattice constants for the rectangular unit cell extracted from the STM image in Fig. 4a are $a = 10\pm0.6 \text{ Å}$ and $b = 09\pm0.4 \text{ Å}$, $\alpha = 90\pm5^{\circ}$. Since the unit cell is rectangular, this structure of BP2 SAMs can be assigned as the $(2\sqrt{3}\times3)$ superstructure. Along the line B that is running along the substrate

<211> direction, every second molecule has the same topographic height. Since the unit cell consists of four molecules, the real density for the adsorbed molecule was calculated to be 21.6 Å² per molecule. On the basis of STM observation, we propose in Fig. 4c a schematic structural model for this phase. In this model, we propose that the topographically higher molecules preferentially sat on the sites located between the on top-bridge sites of the Au(111), whereas molecules with lower topographic heights are adsorbed on the bridge sites of Au(111). This structure is similar to the structure of β-phase observed at RT, the only difference is that at RT the molecule located in the center of the unit cell does not have the same topographic height as those located on the edges of the unit cell, although, the unit cell has the same dimensions and same molecular-area in both cases. We expect the two structures to be identical. It is possible that lack of resolution for SAMs prepared at RT has led to inaccuracy in our determination of topographical heights of the adsorbed molecules. Therefore, hereafter, we will refer to the phase observed in region B as β -phase.

The details of the molecular organization of BP2 on Au(111) in the domains observed in region A are revealed in the higher-resolution STM displayed in Fig. 4d

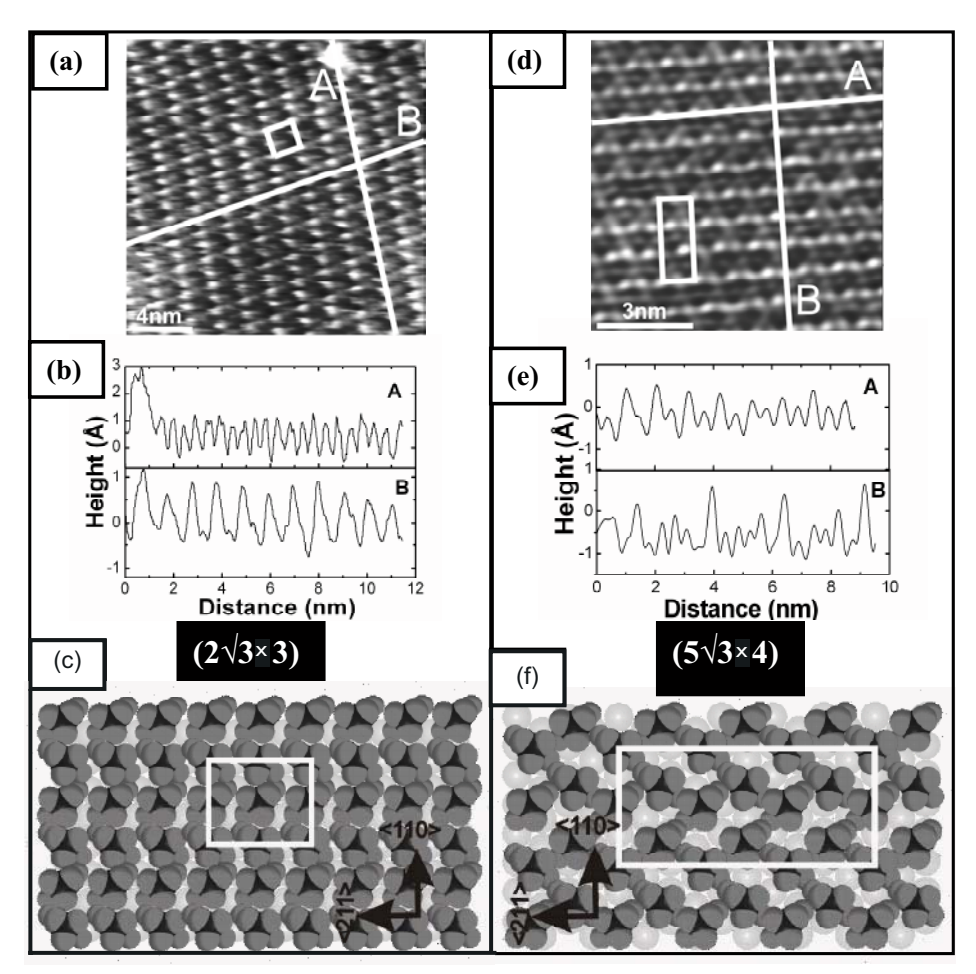


Figure 4. (a) and (d) Constant-current STM images showing the gold surface after immersing into 100 μM ethanolic solution of BP2 at 343 K for 2 h. The rectangular unit cells of the (2√3×3) and (5√3×4) structures are marked in (a) and (d), respectively; (b) and (e) cross-sectional height profiles along the lines A and B labeled in (a) and (d), respectively; (c) and (f) top views of (2√3×3) and (5√3×4) models, respectively. Tunneling parameters: (a) U= 530 mV: 148 pA and (d) U= 530 mV: 148 pA.

and the cross-sectional profiles placed in Fig. 4e. In this phase (y-phase), BP2 molecules form a structure described by a rectangular unit cell. From the crosssectional height profiles along the lines A and B labeled in the STM image Fig. 4d every second and sixth row of molecules have the same topographical heights. The dimensions of the unit cell for the monolayer y-phase have been derived from the line scans taken for a single domain as shown in Figs. 4d and e. Along line A, the lateral repeat distance between the nearest-neighbor brighter molecules is 10.8 Å, whereas along line B it amounts to 25 Å. The angle between the lines A and B is measured to be 90±3°. A comparison of the dimensions and orientation of such a rectangular unit cell with underlying substrate lattice suggests the presence of a $(5\sqrt{3}\times4)$ structure which is the closest structure commensurate with a Au(111) substrate. The highresolution images of the γ-phase show the presence of 12 molecules per unit cell, corresponding to an area per

molecule of 24.03 Ų. A possible molecular ordering in a simple model of ($5\sqrt{3}\times4$) structure is shown in Fig. 4f. In this model, the height modulation between the adsorbed molecules observed in the STM images is assumed to arise from the use of multiple adsorption sites by sulfur atoms on Au(111). The brighter molecules in the STM image are assumed to adsorb on on-top sites of the underlying Au(111) substrate, while darker molecules are proposed to adsorb on the bridge and hcp-hollow sites.

3.2.3. Long-Immersion Times at 343 K

The STM data which were recorded for samples of BP2 monolayer on Au(111) prepared from ethanolic solution at 343 K with immersion time of 3 days are summarized in Fig. 5. Data acquired at larger scale are presented in Fig.5a. The image clearly shows at a glance the existence of cracks and etch-pits similar to those previously observed is the size of the pits has not been affected

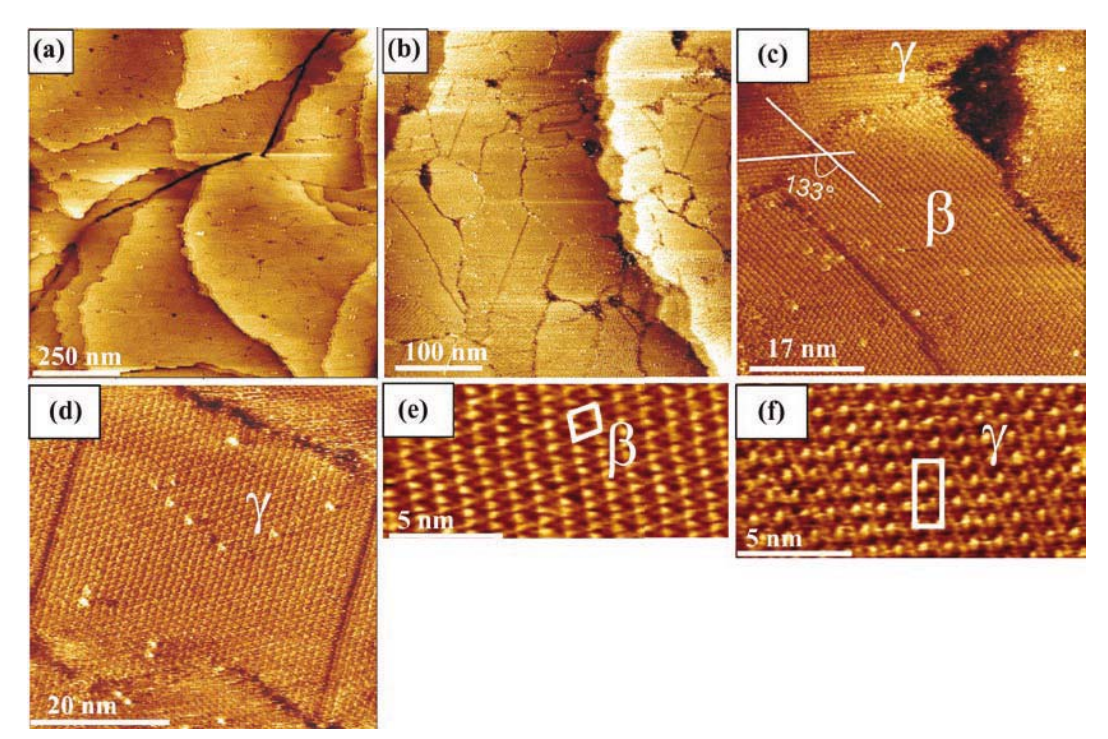


Figure 5. (a)-(f) constant-current STM images showing the gold surface after immersion in 100 μ M ethanolic solution of BP2 at 343 K for 72 h. The rectangular unit cells of the ($2\sqrt{3}\times3$) and ($5\sqrt{3}\times4$) structures are marked in (e) and (f).

by the longer incubation time, remaining at a constant ~15-50 nm, but the boundary-edges of the pits have become smoother. Small islands with height 2.4 Å are again seen in the SAMs but their numerical abundance is dramatically lower. The size of the ordered domains has increased significantly from that observed for the earlier sample, which had been immersed for only 2 h in BP2-solution. In some cases domain in sizes up to 200 nm are observed (see Figs. 5b-d).

No structural changes were observed as a result of increasing the immersion time from 2 h to 3 days at 343 K. Two ordered phases, β -and γ -phases, are again observed to coexist in the SAMs (see Figs. 5e-f). As before, both phases are stable, occupy similar sample areas, and have constant sizes and shapes over time.

3.2.4. Short-Immersion Time at 348 K

Interestingly, immersion of gold substrate into ethanolic solution of BP2 at 348 K results in surface morphology of the SAMs significantly different to that observed for samples prepared at RT and at 343 K (see Figs. 6a-c). In contrast to our expectation of a smooth surface devoid of any SAM defects such as etch-pits or cracks, triangular etch-pits are observed to cover the most gold substrate. The size of the triangular etch-pits ranges from 2-5 nm. This size is comparable to that observed for n-alkanethiols or aromatic thiols at RT.

Small parts of the STM images presented in Figs. 6b and c are covered by large-elevated islands, rising about 0.5 Å above the neighbouring regions. Their size varies from 5-150 nm. Some of these islands are marked in the STM images by the lined loops. Figs. 6b-d clearly show ordered domain covering these islands. Hereafter, this phase of molecular arrangement will be given the name δ -phase. In the other regions of the STM images, differently ordered domains with different directions are observed to co-exist. In some cases, ordered domains corresponding to the α-phase were observed as in Figs. 6d and e. In Fig. 6e, short ordered domains (marked by white loops) of α-phase are present as bright-rods of molecules separating dark-rows. In some cases, the bright-rods are randomly overlapped (see the arrows in Fig. 6e) with each other.

For a detailed analysis of the δ -phase structure, we turn to the high-resolution images displayed in Figs. 6f-h and Fig. 7a. The first characteristic aspect of this structure is the appearance of densely packed rows of molecules, which vary in STM contrast. Fig. 7b shows cross-sectional height profiles along the lines A, B, and C labeled in (a). Along the line A, there are pairs of molecules with the same topographic height. The nearest neighbor brighter molecules spacing is 8.65 Å, which is three times the substrate lattice constant. Therefore, the molecular array along the line A ran in the [110], *i.e.*, nearest-neighbor (NN), direction of the Au(111) surface.

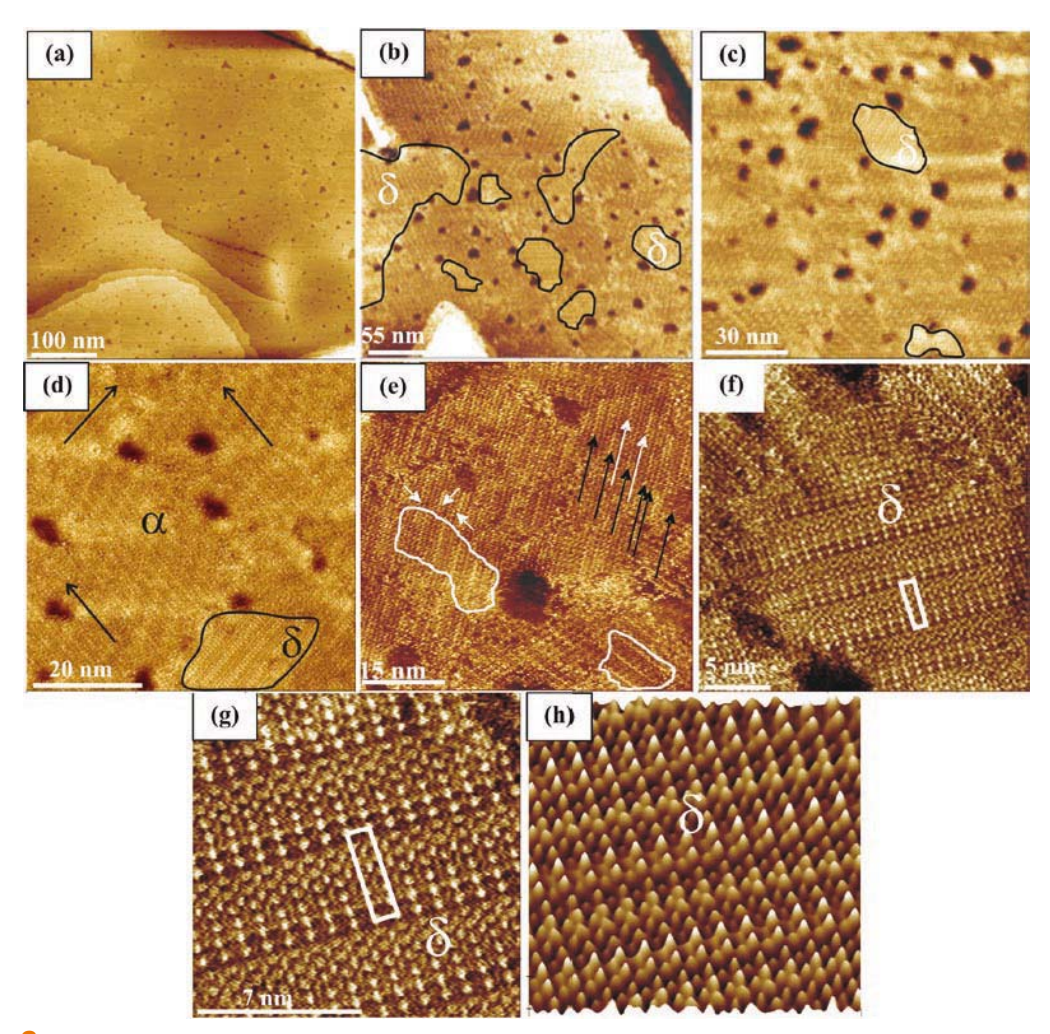


Figure 6. (a)-(g) constant-current STM images showing the gold surface after immersion into 100 μM ethanolic solution of BP2 at 348 K for 2 h. The regions confined by the loops in (b-d) show the δ-phase. The unit cell of the (7√3×3) structure is marked by rectangles in (f) and (g); (h) a 3-D representation of image showing (7√3×3) structure of BP2 SAMs. (a) U= 950 mV; I= 450 pA, (b) U=950 mV; I= 450 pA, (c) U= 950 mV; I= 450 pA, (d) U= 750 mV; I= 350 pA, (e) U= 750 mV; I= 337 pA, (f) U= 450 mV; I= 150 pA, (g) U=450 mV; I= 137 pA, (h) U= 450 mV; I= 137 pA.

Along the lines B and C, every sixth molecule has the same topographic height (i.e., five different variations in contrast for the adsorbate organic thiol BP2 molecules). The intensity of the contrast along the line B appears lower than that observed along the line C, as can be seen in Fig. 7b. The distance between the brighter molecules in the first row and the corresponding one in the second row is 35 Å, which is seven times the $\sqrt{3}a$ distance. Therefore, the straight arrays of the molecules along the lines B and C are perpendicular to the atomic rows and parallel to the $\sqrt{3}$ direction, such as [121]. The adstructure of BP2 exhibits a rectangular primitive unit cell with dimensions of 8.65 × 35 Å. The unit cell, which contains twelve molecules, can be described as $(7\sqrt{3}\times3)$ structure. Thus, the area occupied by a single molecule amounts to 25.25 Å². In Fig. 7c, we propose a schematic model showing the $(7\sqrt{3}\times3)$ structure.

In addition to the $(7\sqrt{3}\times3)$ structure observed in δ -phase, the $(5\sqrt{3}\times3)$ structure (α -phase) is observed as mentioned above. The STM image displayed in Fig. 7d and the cross-sectional profiles shown in Fig. 7e summarize this structure. A model representing this structure is shown in Fig. 7f. The $(5\sqrt{3}\times3)$ and $(7\sqrt{3}\times3)$ structures will be compared in the discussion section.

3.2.5. Long-Immersion Times at 348 K

Astonishingly, increasing the immersion time to 3 days at 348 K results in dramatic changes to the surface morphology of the resulting final structures. Data acquired at larger scale are presented in Fig. 8a. Compared to SAMs prepared after short immersion period (2 h), the density of the vacancy islands increased significantly and their size remains within the range 2-5 nm. Under these preparation conditions, at least three different phases

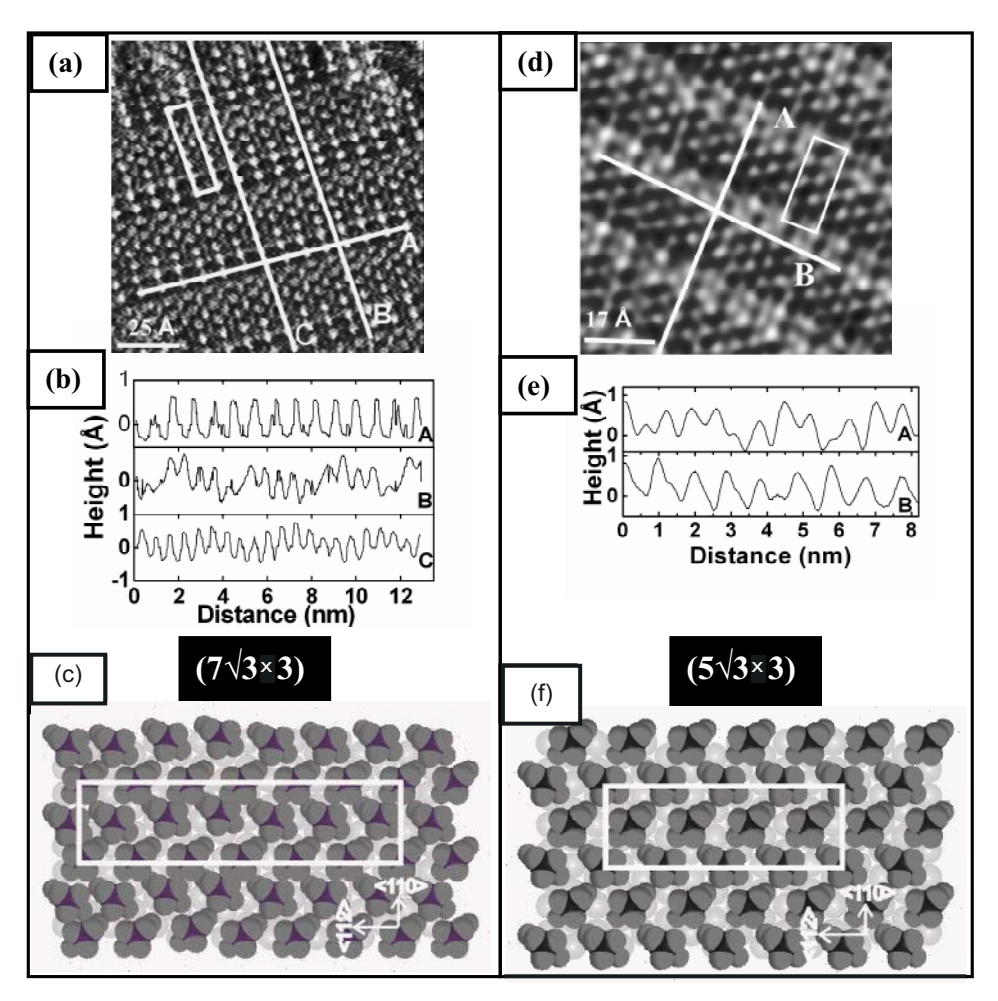


Figure 7. (a) and (d) constant-current STM images showing the gold surface after immersion into 100 μM ethanolic solution of BP2 at 348 K for 2 h. The unit cells of (7√3×3) and (5√3×3) structures are marked by the squares in (a) and (d), respectively; (b) and (e) cross-sectional height profiles along the lines A, B, C and A, B labeled in (a) and (d), respectively; (c) and (f) top views of (7√3×3) and (5√3×3) models, respectively. Tunneling parameters: (a) U= 450 mV; I= 137 pA and (d) U= 550mV; 150 pA.

could be differentiated, namely, $\alpha\text{-phase}$, $\epsilon\text{-phase}$, and a new phase (hereafter $\Phi\text{-phase}$). All these phases can be seen together in the STM presented in Fig. 8b. As can be seen $\alpha\text{-phase}$ forms only a small portion of the surface, whereas, $\epsilon\text{-phase}$ and $\Phi\text{-phase}$ cover almost equal large areas of the SAM. Figs. 8c and f show $\Phi\text{-phase}$ with domains on three equivalent high-symmetry directions. The domains have an average size of 10-60 nm. This phase is characterized by the presence of the previously described cloud-like features. The high density of these disordered areas made it very difficult to determine the exact structure of the $\Phi\text{-phase}$.

The STM images which are displayed in Figs. 8d, e and g show the ϵ -phase. The height profiles along the lines A and B (see Fig. 8g) reveal that there is not just a single value for the distance between the molecules along the line B but a single value is measured for the

long axis of the unit cell along the line A. In the line scan labeled B, which runs along the <110> direction, the intermolecular distances varied between 5 Å and 6.5 Å, with an average equal to 5.75 Å. Along the line labeled A, along the <112> direction, the intermolecular distance is equal to 20 Å. Therefore, the average distances between molecules along the <110> and <211> directions amount to 5.8±0.8 and 20±0.7 Å, respectively. The bases of ϵ -phase structure can, thus, be described as a rectangular ($4\sqrt{3}\times2$) lattice. The unit cell consists of four molecules; therefore, the area per molecule equals 28.9 Ų. A schematic model showing the ϵ -phase structure is presented in Fig. 8i.

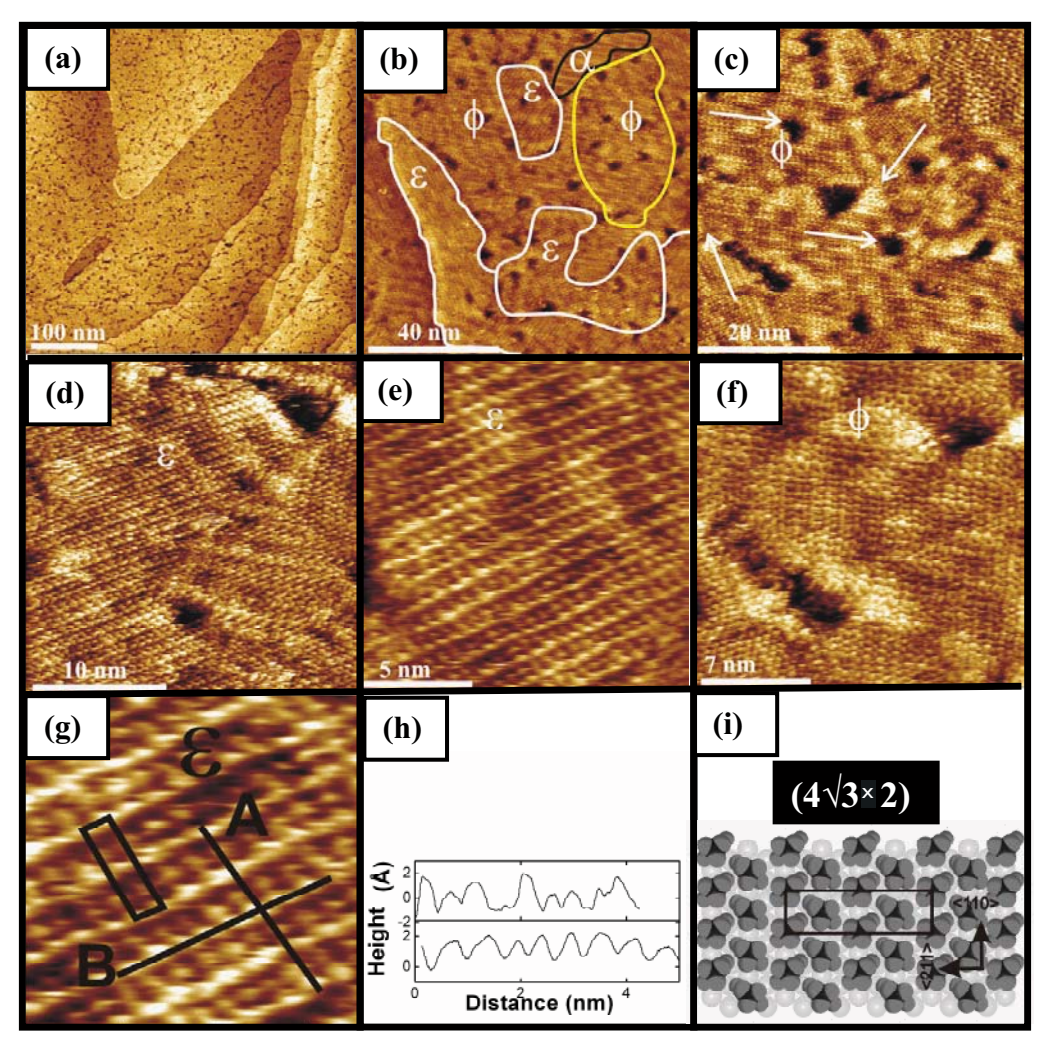


Figure 8. (a-g) constant-current STM images showing the gold surface after immersion into 100 μM ethanolic solution of BP2 at 348 K for 72 h. The arrows in (c) show the different directions of the φ-phase domains. The unit cell of the (4√3×2) structure is marked by the rectangular in (g). (h) cross-sectional height profiles along the lines A and B labeled in (g). (i) top views of (4√3×2) model. (a) U= 1000 mV; I= 501 pA, (b) U= 1000 mV; I= 501 pA, (c) U= 550 mV; I= 350 pA, (d) U= 550 mV; I= 300 pA, (e) U= 531 mV; I= 200 pA, (f) U= 531 mV; I= 150 pA, (g) U=531 mV; I= 150 pA.

4. Discussion

In this work, the effects of the preparation temperature on BP2 film were studied at four different temperatures, namely 298, 333, 343, and 348 K. At all preparation temperatures our STM results indicated the presence of highly ordered monolayers. The STM images recorded at room and elevated temperatures revealed significant differences in the surface morphologies and in the shape or in the size of the unit cell. One of the features common to all SAMs at different temperatures is the etch-pits appearing as dark islands in the STM images. As previously explained [46], these etch-pits are vacancy islands in the topmost layer of the gold surface formed via a corrosion process during thiol adsorption. Comparison of the SAMs prepared at RT with those

formed at elevated temperatures reveals a pronounced dependence of the size and shape of the etch-pits on the preparation temperature. The average domain size was also found to depend significantly on the preparation temperature. With the exception of SAMs prepared at 348 K, our results revealed a pronounced increase in size and a corresponding decrease in the numerical abundance of the etch-pits with increasing preparation temperature, due to the Ostwald ripening process [23,32,40]. The average domain size also increases to a large extent with increasing preparation temperature. At RT and at 333 K domains exhibited sizes in the range 5-25 nm and 5-40 nm (not shown), respectively, whereas, domains of size 150-200 nm were formed at elevated temperatures (343 K). In the SAMs prepared at 348 K, results differed markedly from our expectations.

In particular, etch pits were abundantly present where we had expected only a few. The size and density of the etch-pits for SAMs prepared at 348 K were found to be similar to those observed for thiols on Au(111) at room temperature. For SAMs prepared at 348 K, the size of the ordered domains was found to be 50-150 nm. This value is comparable to that observed for SAMs prepared at 343 K. As yet we do not have an explanation accounting for this unclear and bizarre behavior for BP2 SAMs at 348 K. One possibly important factor could be that the preparation temperature, 348 K, is close to the boiling-point of the solvent (ethanol) used in this work. Therefore, the solution may have had a higher effective concentration of BP2 due to the evaporation of the solvent molecules.

With increasing preparation temperature, phase transitions to new phases having structures different from those observed in SAMs made from higher homologues BP4 and BP6 were observed to take place. The different phase transitions identified are ((5√3×3) [27.05 Å²] and $(2\sqrt{3}\times3)$ [21.6 Å²] at RT & 333 K \rightarrow ((5 $\sqrt{3}\times4$) [24.06 Å²] and $(2\sqrt{3}\times3)$ [21.6 Å²] at 343 K \rightarrow $((7\sqrt{3}\times3)$ [25.25 Å²], $(4\sqrt{3}\times2)$ [28.9 Å²], and $(5\sqrt{3}\times3)$ [27.05 Å²]) 348 K. It is obvious that increasing the preparation temperature to 348 K results in the formation of new phases having lower packing density. At 348 K, The average molecular area in three phases is 27.06 Å2. In this case, we assumed that the three phases are covering equal portions of the BP2-SAM. At 343 and 298 K, the average molecular areas were calculated, under the same assumption, to be 24.08 and 24.3 Å², respectively. The most densely packed phases are these observed for samples prepared at temperatures less than 343 K. In previous studies [40,44], it has been reported that annealing the SAMs at elevated temperatures or preparation the SAMs from hot solutions causes phase transition(s) to new phase(s) with a lower packing density. Comparison of our data for SAMs prepared at 348 K with those prepared at lower temperatures is in clear agreement with this previously reported trend.

The effect of the immersion time on the resulting BP2-SAMs was also examined in this work. Three different immersion times were taken at each temperature; short (2 h) and long (1 day and 3 days). Our results showed that increasing the immersion time does not significantly affect the size of the etch-pits, size of the domains, or even the molecular packing density of the molecules (except for SAMs prepared at 348 K). The SAMs prepared at RT with short immersion periods exhibited a regular arrangement of the etch-pits with separation distances of 13 ± 2 and 7 ± 1 nm. The period of fcc-bridge-hcp-bridge-fcc is 6.3 nm and 6.3 nm×2/ $\sqrt{3}$ =7.3 nm with 120° bending on the herringbone turns, which is equal

to the spacing of the etch-pits within a row. In addition, the periodicity of the zig-zag herringbone turns in the ideal monodomain has been reported to be 7.3×14 nm [47,48], so that our STM images strongly suggest that the etch-pits sites are located at the herringbone corners of the Au(111)-22× $\sqrt{3}$ surface reconstruction.

For samples prepared at RT at all immersion times, two stable phases have been observed, namely, αand β -phases with $(5\sqrt{3}\times3)$ and $(2\sqrt{3}\times3)$ structures, respectively. The α-phase has been also observed for samples prepared at 333 K at low and high immersion times and at 348 K after short immersion time (2 h). The samples prepared at 343 K exhibited the β-phase at all immersion times. In all cases, α-phase was found to coexist with an additional phase(s). In this phase, the rows of molecules forming the short lattice of the $(5\sqrt{3}\times3)$ unit cell run along the <110> direction and those forming the long lattice (5 $\sqrt{3}$) run along the <211> direction. By considering the van der Waals dimensions of the molecule (a cross-sectional area of 21.1 Å² for the phenyl rings) and the area per molecule (27.05 Å²) in the $(5\sqrt{3}\times3)$, the biphenyl axes should be tilted away from the surface normal. The tilt angle of the biphenyl axis in the α -phase is estimated as arcos (21.1/27.05)= 38.7° from the surface normal. BP2 showed evidence of different heights of the molecules within a unit cell. Although the accurate number of molecules appearing at different heights depends rather on the tunneling conditions, we observed, as discussed in detail in earlier publications [32], at least four different heights within a unit cell. Significant differences in height between the different molecules in the unit cell are attributed to different conductivities of the molecules resulting from different S-atom adsorption sites. A structural model for this phase is shown in Fig. 7f. The same structure was observed for TPn, n=even [23] and BPn, n = even systems [32,40] at 298 K and 343 K. Here we point out that in [40], the SAMs of BP2 were prepared at RT, and then annealed at 343 K, whereas the SAMs in this work were directly prepared from hot solution at 343 K. This difference in the procedure of sample preparation can account for the absence of the (5√3×3) structure in our results for samples prepared at 343 K.

β-phase with the structure ($2\sqrt{3}\times3$) was also observed in SAMs prepared at 343 K at all immersion times. In this phase, the $2\sqrt{3}$ -based lattice is found to run along <211>, while the short lattice of the unit cell (3) runs along the <110> direction. The high resolution images showing this phase reveal the presence of four molecules per unit cell, corresponding to an area per molecule of 21.6 Ų. Compared to the 27.05 Ų for ($5\sqrt{3}\times3$) phase, this corresponds to a 25.2% higher packing density. Three different heights for different molecules have

been observed per unit cell. As in $(5\sqrt{3}\times3)$ structure, this difference in the heights was attributed to the different adsorption sites of S-atom and to the herringbone-like arrangement of the phenyl planes. The tilt angle of the molecules is estimated to be 12.5° with respect to the surface normal. A schematic model showing the $(2\sqrt{3}\times3)$ structure is shown in Fig. 4c.

In addition to the β -phase, a new phase (y-phase) was observed for SAMs prepared at 343 K after short and long immersion times. The y-phase has a rectangular unit cell with $(5\sqrt{3}\times4)$ structure. The unit cell consists of twelve molecules corresponding to an area per molecule of 24.06 Å2. On the basis of the vdW dimensions of the BP2 molecules, a tilt angle of 28.4° is estimated. A structural model for this phase is shown in Fig. 4f. In this structure, the short and long lattices of the unit cell are aligned along the <110> and <211> directions, respectively. When comparing the $(2\sqrt{3}\times3)$ and $(5\sqrt{3}\times4)$ structures, we find that in the $(2\sqrt{3}\times3)$ structure, every second row of molecules running along the <211> direction shows the same height in the STM images, while in the $(5\sqrt{3}\times4)$ structure, every sixth molecule along the substrate <211> direction has the same topographical height.

In the $(5\sqrt{3}\times4)$ structure, the distance between the bright features along the <211> direction is about 25 Å, compared with a distance of 10 Å in the $(2\sqrt{3}\times3)$ structure. Moreover, the distance between nearest bright features along <110> directions in the $(5\sqrt{3}\times4)$ and $(2\sqrt{3}\times3)$ structures are 11.56 and 8.6 Å, respectively. This implies that the two structures are almost identical apart from some expansion in the short and long lattices of the $(5\sqrt{3}\times4)$ structure. The β - and γ -phases have not previously been reported for the BP2-Au(111) system.

Two different phases were observed for the SAMs prepared at 348 K after short immersion times. The previously observed α-phase and a new phase labeled in the STM images by δ -phase. In the δ -phase a $(7\sqrt{3}\times3)$ structure was observed, which has not previously been reported. The unit cell of this structure contains twelve molecules, with its molecules occupying an area of 25.25 Å² per molecule. In this structure, at least five different heights for the adsorbates were resolved per unit cell. The tilt angle of the molecules from the surface normal in the δ -phase is estimated to be 33.3°. On the basis of the STM results, we propose a schematic model explaining the $(7\sqrt{3}\times3)$ structure. The model is presented in Fig. 7c. In this model, the phenyl planes are orientated in a herringbone fashion along the [121] direction of the gold surface. The five different variations in contrast of the twelve molecules comprising the unit cell have been attributed to different adsorption sites of the sulfur headgroups on the Au(111) surface such as

triple-hcp hollow, fcc, bridge, near-top, and top sites. When comparing the $(5\sqrt{3}\times3)$ structure with the $(7\sqrt{3}\times3)$ one, we find that they share some structural features: specifically that every second row of molecules running along the <110> direction shows the same height in the STM images. For both structures, the distance between equivalent rows of molecules amounts to about 8.67 Å. In addition, for $(5\sqrt{3}\times3)$ structure every fourth row of molecules oriented parallel to the <112> direction exhibits the same height. The corresponding unit cell length amounts to 25 Å along the <112> direction, corresponding to an intermolecular distance of 6.25 Å, which is significantly larger than the value 5 Å. In the $(7\sqrt{3}\times3)$ structure, every sixth molecules along the <112> direction exhibits the same height. The unit cell length along this direction amounts 35 Å. This value matches an intermolecular distance of 5.8 Å. Compared to the $(5\sqrt{3}\times3)$ structure, the unit cell of the $(7\sqrt{3}\times3)$ structure is expanded along the <112> direction (from 25 to 35 Å) and the spacing of the molecules along this direction is decreased slightly from 6.25 to 5.8 Å. This decreased spacing is associated with a length increase of the unit cell to $7\sqrt{3}$ from $5\sqrt{3}$.

For samples prepared at 348 K after long immersion times (3day), three different phases are observed α -, ϵ -, and Φ -phases. It is clear that the SAMs of BP2 prepared at 298, 333 K, and from hot solution (348 K) are accompanied by α -phase. The Φ -phase is an ordered phase and the three equivalent high-symmetry directions can be seen, but its structure could not be determined. In contrast to Φ -phase, the unit cell dimensions of ϵ -phase were easily determined from different STM images to fit nicely with the ($4\sqrt{3}\times2$) structure. The area per molecule was calculated to be 28.9 Ų. In this phase, the molecules are estimated to tilt away from the surface normal by 43.1°.

The growth of SAMs made from $\mathrm{CH_3-(C_6H_4)_2-SH}$ (BPT) has previously been studied using STM(30). For samples prepared after short immersion times (3 min to 3 h), striped structures are observed, where the molecules are orientated with their axes parallel to the surface. Such molecular structures have not been observed for BP2-SAMs. Even after short immersion times, the BP2 molecules stand up with biphenyl axes almost perpendicular to the surface. The absence of the striped phases in BP2-SAMs is attributed to the free joint groups (-CH₂ units) that exist in the molecular structure of BP2.

The main structures observed in this and in the previous studies on BP2 SAMs are summarized in Table 1. In a recent study [45], BP2 films grown from solution at RT and annealed at 337 K for 2 h were investigated. Two structures have been reported: the quadratic $(4 \times 6 \sqrt{3})$ and the centered $(4 \times 6 \sqrt{3})$ structures.

Table 1. Structures Adopted by BP2-SAMs at Different Deposition Temperatures.

| Structure | Deposition Temperature | Immersion Time | Molecular area, (Ų) | Reference |
|-------------------------------|--------------------------------|-------------------|---------------------|-----------|
| Rec (5√3×3) | RT and 343 K | 24 h | 27.05 | 43, 32 |
| (4×6√3) quadratic | RT then annealed 2 h at 337 K | - | 34.68 | 44 |
| $(4\times6\sqrt{3})$ centered | RT then annealed 2 h at 337 K | - | 34.68 | 44 |
| (2√3×2) | RT then annealed 15 h at 417 K | - | 28.70 | 43 |
| Rec (5√3×3) | RT | 2 h & 24 h & 72 h | 27.05 | This work |
| Rec (2√3×3) | RT | 2 h & 24 h & 72 h | 21.60 | This work |
| Rec (2√3×3) | 343 K | 2 h & 24 h & 72 h | 21.60 | This work |
| Rec (5√3×4) | 343 K | 2 h & 24 h & 72 h | 24.03 | This work |
| Rec (7√3×3) | 348 K | 2 h | 25.28 | This work |
| Rec (5√3×3) | 348 K | 2 h | 27.05 | This work |
| Rec (4√3×2) | 348 K | 24 h | 28.70 | This work |

The area occupied by a single molecule was calculated to be $34.68~\text{Å}^2$ for both structures. Our results collected for SAMs prepared at 333~K and 343~K failed to show the existence of such structures. Moreover, these structures have a much lower molecular density than those we observed in the present study. The reasons for the differences between these observations and our results in this study are still unclear. It should be noted however, that the preparation conditions were different and that the resolution of the previously reported STM data was rather inferior to the data presented here.

More recently [44], BP2-SAMs on Au(111) were studied using different surface techniques. In their STM studies for samples prepared at RT and then annealed for 15 h at elevated temperatures ≥373 K, a phase transition from $(5\sqrt{3}\times3) \rightarrow (2\sqrt{3}\times2)$ was observed. In the $(2\sqrt{3}\times2)$ structure, the area per molecule was calculated to be 28.70 Å². Moreover, variation in the intermolecular distances along the short lattice of the unit cell was observed. Actually, the presence of the $(5\sqrt{3}\times3)$ structure at temperature ≥373 K is in accordance with our results in which the $(5\sqrt{3}\times3)$ structure still exist at 348 K. Moreover, the $(2\sqrt{3}\times2)$ structure is identical to the $(4\sqrt{3}\times2)$ structure we observed at 348 K after long immersion time. Both proposed structures have equal molecular area (28.70 Å²) and variation in the intermolecular distances along the short lattice of the unit cell. The only difference between the two structures is the periodicity length along the long axes of the unit cell. In their study, the average distance between molecules along the <211> direction amounts to 10±0.6 Å, whereas, a value of 20±0.7 Å was found in our results. As in the $(2\sqrt{3}\times2)$ structures, the molecules in the $(4\sqrt{3}\times2)$ structure repeat their topographic height every 10 Å along <112> direction but a slight lateral displacement in the position of the molecules was observed every second row in

the $(4\sqrt{3}\times2)$ structure. Therefore, this phase is better described by $(4\sqrt{3}\times2)$ structure than $(2\sqrt{3}\times2)$.

5. Conclusion

SAMs of BP2 on Au(111) were investigated at different preparation temperatures. At each temperature, different samples were prepared for different immersion times. The STM imaging revealed that BP2 molecules on Au(111) form highly ordered SAMs at room and elevated temperatures. In samples prepared at room temperature and at 333 K after short and long immersion times, the BP2 molecules form two distinct phases; α- and β-phases. In these phases, the $(5\sqrt{3}\times3)$ and $(2\sqrt{3}\times3)$ structures were observed, respectively. Increasing the solution temperature to 343 K results in the formation of a new structure described by $(5\sqrt{3}\times4)$ structure. Further increase of the preparation temperature to 348 K for short immersion time causes a phase transition to a new phase assigned as the $(7\sqrt{3}\times3)$ superstructure. Furthermore, increasing immersion time from 2 h to 3 days at 348 K results in $(7\sqrt{3}\times3) \rightarrow (4\sqrt{3}\times2)$ phase transition through a decrease of packing density. From this study, we demonstrated that solution temperature and immersion periods of the substrate into the thiol solution play very important roles in controlling the two dimensional SAM structure of BP2. Additionally, our STM results will be very useful in understanding the selfassembly phenomena of BP2 conjugated molecules on Au(111) from a pure solvent.

Acknowledgment

The author gratefully acknowledges the short-term research fellowship supported by the DFG and TTU (Tafila Technical University) for its partial support.

References

- [1] M.A. Reed, C. Zhou, C.J. Muller, T.P. Burgin, J.M. Tour, Science 278, 252 (1997)
- [2] B.A. Mantooth, P.S. Weiss, Proc. IEEE 91, 1785 (2003)
- [3] C.P. Collier, J.O. Jeppensen, Y. Luo, J. Perkins, E.W. Wong, J.R. Heat, J.F. Stoddart, J. Am. Chem. Soc. 123, 12632 (2001)
- [4] S. Flink, F. van Veggel, D.N. Reinhoudt, Adv. Mater. 12, 1325 (2000)
- [5] T. Felgenhauer, C. Yan, W. Geyer, H.T. Rong, A. Goelzhaeuser, M. Buck, Appl. Phys. Lett. 79, 3323 (2001)
- [6] J. Scherer, M.R. Vogt, O.M. Magnussen, R.J. Behm, Langmuir 13, 7045 (1997)
- [7] R.K. Smith, P.A. Lewis, P.S. Weiss, Surf. Sci. 75, 1 (2004)
- [8] K.L. Prime, G.M. Whitesides, J. Am. Chem. Soc. 115, 10714 (1993)
- [9] K. Seo, E. Borguet, J. Phys. Chem. C 111(17), 6335 (2007)
- [10] B.S. Kim, J.M. Beebe, Y. Jun, X.-Y. Zhu, C.D. Frisbie, J. Am. Chem. Soc. 128(15), 4970 (2006)
- [11] W. Chen et al., J. Phys. Chem. B. 110(51), 26075 (2006)
- [12] A. Jakubowicz, H. Jia, R.M. Wallace, B.E. Gnade, Langmuir 21(3), 950 (2005)
- [13] P. Jiang, A. Nion, A. Marchenko, L. Piot, D. Fichou, J. Am. Chem. Soc. 128(38), 12390 (2006)
- [14] J. Noh, Y. Jeong, E. Ito, M. Hara, J. Phys. Chem. C 111(6), 2691 (2007)
- [15] H. Noda, Y. Tai, A. Shaporenko, M. Grunze, M. Zharnikov, J. Phys. Chem. B 109(47), 22371 (2005)
- [16] P. Cyganik, M. Buck, J.D.E.T. Wilton-Ely, C. Woll, J. Phys. Chem. B 109(21), 10902 (2005)
- [17] V. Ganesh, V. Lakshminarayanan, J. Phys. Chem. B 109(34), 16372 (2005)
- [18] W.S. Hu, Y.T. Tao, Y.J. Hsu, D.H. Wei, Y.S. Wu, Langmuir 21(6), 2260 (2005)
- [19] T. Weidner, A. Shaporenko, J. Muller, M. Holtig, A. Terfort, M. Zharnikov, J. Phys. Chem. C 111(31), 11627 (2007)

- [20] M.B. Smith, K. Efimenko, D.A. Fischer, S.E. Lappi, P.K. Kilpatrick, J. Genzer, Langmuir 23(2), 673 (2007)
- [21] A. Kanjilal, L. Ottaviano, V. Di Castro, M. Beccari, M.G. Betti, C. Mariani, J. Phys. Chem. C 111(1), 286 (2007)
- [22] R.-F. Dou et al., Langmuir 22(7), 3049 (2006)
- [23] W. Azzam, A. Bashir, A. Terfort, T. Strunskus, C. Woll, Langmuir 22(8), 3647 (2006)
- [24] A. Shaporenko, K. Heister, A. Ulman, M. Grunze, M. Zharnikov, J. Phys. Chem. B 109(9), 4096 (2005)
- [25] D. Kafer, A. Bashir, G. Witte, J. Phys. Chem. C 111(28), 10546 (2007)
- [26] A. Shaporenko, M. Elbing, A. Blaszczyk, C. von Hanisch, M. Mayor, M. Zharnikov, J. Phys. Chem. B 110(9), 4307 (2006)
- [27] C. Fuxen, W. Azzam, R. Arnold, A. Terfort, G. Witte, C. Wöll, Langmuir 17, 3689 (2001)
- [28] R. Arnold, W. Azzam, A. Terfort, C. Wöll, Langmuir 18, 3980 (2002)
- [29] A. Niklewski, W. Azzam, T. Strunskus, R.A. Fischer, C. Wöll, Langmuir 20, 8620 (2004)
- [30] W. Azzam, C. Fuxen, A. Birkner, H.-T. Rong, M. Buck, C. Wöll, Langmuir 19, 4958 (2003)
- [31] W. Azzam, B.I. Wehner, R.A. Fischer, A. Terfort,C. Wöll, Langmuir 18(21), 7766 (2002)
- [32] W. Azzam, P. Cyganik, G. Witte, M. Buck, C. Wöll, Langmuir 19, 8262 (2003)
- [33] G.H. Yang, G.Y. Liu, J. Phys. Chem. B 107, 8746 (2003)
- [34] T. Baunach, D.M. Kolb, Anal. Bioanal. Chem. 373, 743 (2001)
- [35] L. Venkataraman, J.E. Klare, C. Nuckolls, M.S. Hybertsen, M.L. Steigerwald, Nature 442, 904 (2006)
- [36] E. Tran, M. Duati, V. Ferri, K. Mueller, M. Zharnikov, G.M. Whitesides, M.A. Rampi, Adv. Mater. 18, 1323 (2006)
- [37] M. Aslam, N.K. Chaki, J. Sharma, K. Vijayamohanan, Curr. Appl. Phys. 3, 115 (2003)
- [38] A.M. Bratkovsky, P.E. Kornilovitch, Phys. Rev. B 67, 115307 (2003)

- [39] K. Heister, H.T. Rong, M. Buck, M. Zharnikov, M. Grunze, L.S.O. Johansson, J. Phys. Chem. B 105, 6888 (2001)
- [40] P. Cyganik, M. Buck, W. Azzam, C. Wöll, J. Phys. Chem. B 108, 4989 (2004)
- [41] Y.T. Long, H.T. Rong, M. Buck, M. Grunze, J. Electroanal.Chem. 524, 62 (2002)
- [42] T. Felgenhauer, H.-T. Rong, M. Buck, J. Electroanal. Chem. 550-551, 309 (2003)
- [43] S. Frey, H.T. Rong, K. Heister, Y.J. Yang, M. Buck, M. Zharnikov, Langmuir 18, 3142 (2002)
- [44] P. Cyganik, M. Buck, T. Strunskus, A. Shaporenko, G. Witte, M. Zharnikov, C. Wöll, J. Phys. Chem. C 111, 16909 (2007)

- [45] B. Luessem, L. Mueller-Meskamp, S. Karthaeuser, M. Homberger, U. Simon, R. Waser, J. Phys. Chem. C 111(17), 6392 (2007)
- [46] K. Edinger, M. Grunze, C. Wöll, Ber. Bunsenges. Phys. Chem. 101, 1811 (1997)
- [47] J.V. Barth, H. Brune, G. Ertl, R.J. Behm, P.H. Lippel, Phys. Rev. B 42, 9307 (1990)
- [48] D.D. Chambliss, R.J. Wilson, J. Vac. Sci. Technol. B 9, 928 (1991)